8-2018

Bm-iAANAT and its Potential Role in Fatty Acid Amide Biosynthesis in *Bombyx mori*

Ryan L. Anderson
University of South Florida

Matthew R. Battistini
University of South Florida

Dylan J. Wallis
University of South Florida

Christopher Shoji
University of South Florida

Brian G. O'Flynn
University of South Florida, oflynnb@mail.usf.edu

See next page for additional authors

HHS Public Access

Author manuscript

Prostaglandins Leukot Essent Fatty Acids. Author manuscript; available in PMC 2019 August 01.

Published in final edited form as:

Prostaglandins Leukot Essent Fatty Acids. 2018 August ; 135: 10–17. doi:10.1016/j.plefa.2018.06.001.

Bm-iAANAT and its Potential Role in Fatty Acid Amide Biosynthesis in *Bombyx mori*

Ryan L. Anderson, **Matthew R. Battistini**, **Dylan J. Wallis**, **Christopher Shoji**, **Brian G. O'Flynn**, **John E. Dillashaw**, and **David J. Merkler***

Department of Chemistry, University of South Florida, Tampa, FL 33620

Abstract

The purpose of this research is to unravel the substrate specificity and kinetic properties of an insect arylalkylamine *N*-acyltransferase from *Bombyx mori* (*Bm*-iAANAT) and to determine if this enzyme will catalyze the formation of long chain *N*-acylarylalkylamides *in vitro*. However, the determination of substrates and products for *Bm*-iAANAT *in vitro* is no guarantee that these same molecules are substrates and products for the enzyme in the organism. Therefore, RT-PCR was performed to detect the *Bm*-iAANAT transcripts and liquid chromatography quadrupole time-of-flight mass spectrometry (LC-QToF-MS) analysis was performed on purified lipid extracts from *B. mori* larvae (fourth instar, Bmi4) to determine if long chain fatty acid amides are produced in *B. mori*. Ultimately, we found that recombinant *Bm*-iAANAT will utilize long-chain acyl-CoA thioesters as substrates and identified *B*m-iAANAT transcripts and long-chain fatty acid amides in Bmi4. Together, these data show *Bm*-iAANAT will catalyze the formation of long-chain *N*-acylarylalkylamides *in vitro* and provide evidence demonstrating that *Bm*-iAANAT has a role in fatty acid amide biosynthesis in *B. mori*, as well.

Keywords

Arylalkylamine *N*-acyltransferase; Dopamine; Fatty acid amide biosynthesis; Serotonin

1. Introduction

Fatty acid amides are a family of structurally related lipids, R-CO-NH-R′ (the acyl moiety, R-CO-, is derived from a fatty acid and the R′-NH- moiety is derived from an amine), found in both vertebrates and invertebrates [1–3]. The existence of the *N*-acylamide bond in biology traces back to the identification of hippurate (*N*-benzoylglycine) as a metabolite derived from benzoate in the early 1840's [4,5] and the fatty acid amide bond traces back to the 1870's to the work of J.L.W. Thudicum on sphingomyelin and other brain ceramides [6].

*Corresponding Author: Dr. David J. Merkler, Department of Chemistry, University of South Florida, 4202 E. Fowler Ave., CHE 205, Tampa, FL 33620 USA, Phone: 813-974-3579, FAX: 813-974-3203, merkler@usf.edu.

Conflicts of Interest

The authors declare no conflicts of interest.

The best understood member of the fatty acid amide family is *N*-arachidonoylethanolamine (anandamide), the endogenous ligand to the mammalian cannabinoid receptor, CB_1 [7,8]. Based on our knowledge about anandamide [9,10], it is generally thought the fatty acid amides are neuroactive [2,11]. This is consistent with the discovery of oleamide, a sleep-inducing lipid amide, and the existence of a family of long-chain *N*-acylethanolamines in the mammalian brain [12–14]. Fatty acid amides are found in invertebrates, as well [15–20], but likely serve different functions in these organisms relative to mammals. For example, *Drosophila melanogaster* do produce fatty acid amides [17–19], but do not express the cannabinoid receptors [21].

Much remains unknown about the fatty acid amides: many have no clearly defined physiological function, details regarding their metabolism remain elusive (biosynthesis, degradation, and cellular transport), and the receptor(s) targeted by most are unidentified [1–3,22]. One focus of our research has been on the identification and characterization of enzymes involved in fatty acid amide biosynthesis and melding *in vitro* substrate specificity data with metabolomic data [23,24]. We have proposed *N*-acyltransferases operate in fatty acid amide biosynthesis: acyl-CoA + amine → *N*-acylamide + CoA-SH (Fig. 1) [25]. Such *N*-acyltransferases are likely members of the GCN5-related superfamily of *N*-acetyltransferases (GNATs) [26,27], which would accept long-chain acyl-CoA thioesters as substrates. Examples of GNAT enzymes utilizing long-chain acyl-CoA thioesters as substrates include *N*-myristoyl transferase [28], glycine *N*-acyltransferase-like 2 [29], and arylalkylamine *N*-acyltransferase-like 2 (AANATL2) [23].

We have employed *Drosophila melanogaster* and mouse neuroblastoma $N_{18}TG_2$ cells in our previous work on the fatty acid amides. Each of these produce fatty acid amides [1,16–18,24,30,31] and both express an *N*-acyltransferase that could have a role in fatty acid amide biosynthesis [23,24]. In *D. melanogaster*, we found the expression profiles of AANATL2 matched well with the metabolomic data showing the presence of the long-chain *N*-acyldopamines and *N*-acylserotonins. Work carried out *in vitro* demonstrated *D. melanogaster* AANATL2 would catalyze the production of long-chain *N*-acyldopamines and *N*-acylserotonins [23]. In the $N_{18}TG_2$ cells, we demonstrated that siRNA-mediated knock-down of glycine *N*-acyltransferase like 3 (GLYATL3) results in the accumulation of long-chain *N*-acylglycines in these cells. These results are consistent with limited *in vitro* substrate specificity data available for GLYATL3 [24]. In sum, our work and that of Waluk *et al*. [29] strongly suggest *N*-acyltransferases do catalyze key reactions in the fatty acid amide biosynthetic pathway.

We decided to add *Bombyx mori*, the domesticated silkworm, as a model organism for our fatty acid amide studies. *B. mori* is known to express *Bm*-iAANAT, an enzyme catalyzing the acetyl-CoA-dependent *N*-acetylation of amines and exhibiting a wide tissue distribution [32]. Mutation of *Bm*-iAANAT led to melanism and to the accumulation of dopamine in the silkworm [33,34]. A more complete analysis of the substrate specificities of *Bm*-iAANAT seemed warranted to determine if long-chain acyl-CoA thioesters were substrates for this enzyme. If so, the availability of mutants and its broad tissue distribution data point to straightforward metabolomic experiments to evaluate the *in vivo* role of *Bm*-iAANAT in fatty acid amide biosynthesis.

We report, herein, long-chain acyl-CoA thioesters like palmitoyl- and oleoyl-CoA are substrates for *Bm*-iAANAT leading to the formation of fatty acid amides *in vitro*. Also, we find *Bm*-iAANAT accepts many amines as substrates, significantly expanding the list of amine substrates reported for this enzyme [32]. *Bm*-iAANAT is, thus, a "promiscuous generalist" with regards to the acyl-CoA and amine substrates. We identified a set of fatty acid amides in 4th instar larvae of *B. mori*, the first report of these lipid amides in these insects and found *Bm*-iAANAT is expressed in 4th instar larvae. The combination of all our data are consistent with *Bm*-iAANAT functioning in the biosynthesis of fatty acid amides, at least in 4th instar larvae of *B. mori*.

2. Materials and Methods

2.1 Materials

Unless otherwise noted, all reagents were obtained from commercial sources. Codon-optimized *Bm*-iAANAT was purchased from Genscript. Oligonucleotides were purchased from Eurofins MWG Operon BL21 (DE3) *E. coli* cells, XL-10 competent cells, and the *pET28a*(+) vector were purchased from Novagen. PfuUltra High-Fidelity DNA polymerase was purchased from Agilent. XhoI, NdeI, Antarctic phosphatase, and T4 DNA ligase were purchased from New England Biolabs. Kanamycin monosulfate and IPTG were purchased from Gold Biotechnology. ProBond nickel-chelating resin was purchased from Invitrogen. Long and short-chain acyl-CoA thioesters and amine substrates were purchased from Sigma-Aldrich. *N*-Oleoyltryptamine was synthesized from oleoyl chloride and tryptamine essentially as described for the synthesis of *N*-heptanoyltryptamine [35]. All other supplies and materials were of the highest quality available from either Sigma or Fisher Scientific. Spectrophotometric analyses were performed on a Cary 300 Bio UV-Visible spectrophotometer.

2.1 Cloning of Bm-iAANAT

Bm-iAANAT (Accession No. NM_001079654.2) was codon optimized for expression in *E. coli*, with 5′-NdeI and 3′-XhoI restriction sites, included an N-terminal His_6-tag separated from the N-terminal methionine of wildtype enzyme with a 10-amino acid linker (SSGLVPRGSH), and synthesized into a *pUC57* vector. The full-length gene was excised from the *pUC57* vector and ligated into the NdeI and XhoI restriction sites of the *pET-28a* vector. The *Bm-iAANAT- pET28a* vector was then transformed into *E. coli* XL-10 competent cells, plated on a Luria Broth (LB) agar plate supplemented with 50 μg/mL kanamycin and grown overnight at 37°C. A single colony from each vector transformation was cultured overnight in LB media supplemented with 50 μg/mL kanamycin overnight at 37°C. The *Bm-iAANAT-pET28a* plasmid was purified from the overnight cultures using the Promega Wizard Plus SV Minipreps DNA purification kit, sequenced by Eurofins MWG Operon to confirm correct gene insertion, and finally transformed into *E. coli* BL-21 (DE3) cells for the expression of *Bm*-iAANAT.

2.2 Expression and Purification of Bm-iAANAT

The *E. coli* BL-21 (DE3) competent cells containing the *Bm-iAANAT-pET28a* vector were cultured in LB media supplemented with 50 μg/mL kanamycin at 37°C. Once the cultures

reached an absorbance of 0.6 at 600 nm, cells were induced with the addition of 1.0 mM isopropyl β-D-thiogalactopyranoside (IPTG) for 4 hours at 37°C. The final cultures were harvested by centrifugation at 6,000 × g for 10 minutes at 4°C, and pellets were frozen at −80°C for later analysis. Cell pellets were thawed and suspended in Binding buffer: 20 mM Tris pH 7.9, 500 mM NaCl, and 5 mM imidazole. Cells were lysed by sonication and the cellular debris was pelleted by centrifugation at 16,000 × g for 20 minutes at 4°C. The supernatant was retained and loaded onto a 5 mL column of ProBond nickel-chelating resin. The column was washed with 5 column volumes (CVs) of Binding buffer, followed by 10 CVs of Wash buffer: 20 mM Tris pH 7.9, 500 mM NaCl, and 60 mM imidazole. Finally, purified enzyme was eluted from the column in 1 mL fractions with 2–3 CVs of Elution buffer: 20 mM Tris pH 7.9, 500 mM NaCl, and 500 mM imidazole. Fractions were evaluated for purity and protein concentration using 10% sodium dodecyl sulfate polyacrylamide gel electrophoresis (SDS-PAGE) gels and Bradford binding assay, respectively. Fractions containing the purified *Bm*-iAANAT were pooled, dialyzed overnight in 20 mM Tris pH 7.4, 200 mM NaCl, and stored at −80°C.

2.3 Identification of the Amine Substrates for Bm-iAANAT

To identify amine substrates, *Bm*-iAANAT activity was measured using either acetyl-CoA (representative of a short-chain acyl-CoA) or oleoyl-CoA (representative of a long-chain acyl-CoA) separately along with sets of different amines grouped together. The amines included in each group are listed in Table S1 (Supplementary Material). The assay solutions used to measure *Bm*-iAANAT activity from the groups of amines consisted of 300 mM Tris pH 8.0, 150 μM DTNB (5,5′-dithiobis (2-nitro-benzoic acid), Ellman's reagent), 500 μM of either acetyl- or oleoyl-CoA and the all the amines grouped together as shown in Table S1 (Supplementary Material, each amine at 60 mM) at 22°C. Initial velocities were determined by measuring the release of CoA-SH at 412 nm (ε_{412} = 13,600 M^{-1} cm^{-1}) [36], with the reported velocities calculated as the background acyl-CoA thioester hydrolysis rate subtracted from the observed velocity. The rates of background acyl-CoA hydrolysis were determined in absence of *Bm*-iAANAT or after adding heat-denatured (boiled) *Bm*-iAANAT. The background rates of acyl-CoA hydrolysis were the same, within experimental error, for the two control experiments. Any combination of amine group and acyl-CoA displaying a background-corrected rate ≥0.1 μmoles/min/mg was considered a "hit", exhibiting a rate of CoA-SH release ≥3-fold the above background rate. The individual amines within an amine group showing a "hit" were then individually interrogated further at 60 mM in solution with 300 mM Tris pH 8.0, 150 μM DTNB, and 500 μM acetyl-CoA or 500 μM oleoyl-CoA to determine which amines with the group were substrates for *Bm*-iAANAT. Individual amines were considered *Bm*-iAANAT substrates if the rate of CoA-SH release was ≥0.1 μmoles/min/mg above background acyl-CoA hydrolysis rate.

2.4 Determination of Steady-State Kinetic Constants

Steady-state kinetic characterization of *Bm*-iAANAT was assayed by measuring the release of CoA-SH at 412 nm at 22°C under the following conditions: 300 mM Tris pH 8.0, 150 μM DTNB, and different initial concentrations of the substrates: an amine and an acyl-CoA. To determine the apparent kinetic constants for the acyl-CoA thioester substrates, the initial tryptamine concentration was 60 mM while the initial concentration of the desired acyl-CoA

was varied. To determine the apparent kinetic constants for an amine substrate, the initial acyl-CoA concentration was 100 μM while the initial concentration of the amine was varied. The apparent kinetic constants were determined by fitting the resulting initial rate vs. [substrate] data to Equation 1 using SigmaPlot 12.0: v_o represents initial velocity, $V_{max,app}$ is the apparent maximal velocity, $K_{m,app}$ is the apparent Michaelis constant, and [S] is the substrate concentration. Assays were performed in triplicate. The uncertainty for the $(k_{cat}/K_m)_{app}$ values were calculated using Equation 2, where σ is the standard error of the $k_{cat,app}$ and $K_{m,app}$ values [37].

$$v_o = \frac{V_{max,\,app}[S]}{K_{m,\,app} + [S]} \quad \text{Equation 1}$$

$$\sigma\left(\frac{x}{y}\right) = \frac{x}{y}\sqrt{\left(\frac{\sigma_x}{x}\right)^2 + \left(\frac{\sigma_y}{y}\right)^2} \quad \text{Equation 2}$$

2.5 Characterization of the Product Generated by Bm-iAANAT by LC-QToF-MS

The use of Ellman's reagent to measure CoA-SH release from acetyl-CoA or oleoyl-CoA is no guarantee of *N*-acylamide formation. To confirm *N*-acylamide product formation in a reaction catalyzed by *Bm*-iAANAT, 1 mM tryptamine and 500 μM oleoyl-CoA were incubated with 100 μg of purified enzyme for 1 hour in 300 mM Tris pH 8.0. A control lacking enzyme was run in parallel. We determined this ratio of [oleoyl-CoA]/[tryptamine] was ideal for *N*-acylamide production after several optimization experiments because *Bm*-iAANAT can be inhibited by a high concentration of the amine substrate [32]. Following the 1 hr. incubation, the reaction mixture was then passed through a 10 kDa ultrafilter (Millipore) to remove *Bm*-iAANAT. Aliquots (20 μL) of the resulting flow-through solution containing the putative *N*-oleoyltryptamine product from the experiment with enzyme and the control lacking enzyme were injected separately on an Agilent 6540 liquid chromatography/quadrupole time-of-flight mass spectrometer (LC-QTOF-MS) in positive ion mode. The *N*-oleoyltryptamine standard and the enzymatic reaction product characterizations were completed on a Kinetex 2.6 μm C_{18} 100 Å (50 × 2.1 mm) reverse phase column with the following mobile phase gradient with a flow rate of 0.6 mL/min: mobile phase A was 0.1% (v/v) formic acid in water, while mobile phase B was 0.1% (v/v) formic acid in acetonitrile. A linear gradient of 10% mobile phase B increased to 100% B over 5 minutes, followed by a hold of 3 minutes at 100% B for the analysis of the product. The column was then equilibrated with 10% mobile phase B for 10 minutes before subsequent injections. The column was thoroughly washed between injections using the same solvent gradient, but at a flow rate of 1.0 mL/min.

2.6 Detection of Bm-iAANAT Transcripts in 4th Instar Larvae of B. mori via RT-PCR

2.6.1 Silkworm Culture and Isolation of mRNA—*B. mori* eggs were purchased from Carolina Biological and immediately placed into a petri dish upon arrival. Silkworms were

cultured with Silkworm Artificial Dry Diet from Carolina Biological and allowed to grow until the fourth instar: after the larvae had molted three times from their original hatch. Total RNA was extracted using the PureLink® RNA Mini Kit from Invitrogen and the mRNA was then isolated via PolyATtract® mRNA Isolation Systems III from Promega. After the elution of mRNA in nuclease-free water, a 10 kDa centrifugal filter was used to concentrate the heavier nucleic acids (15 min at 12,000 × g). Any traces of remaining genomic DNA were removed using DNase I from Thermo Fisher with the modifications to the recommended protocol, as outlined in Table 1. The reaction mixture was briefly centrifuged, heated at 37°C for 30 minutes, followed by the addition of 2 μL of 50 mM EDTA, and, lastly, heating for another 10 minutes at 65°C to inactivate the DNase I.

2.6.2 Generation of cDNA library and transcripts for Bm-iAANAT and Bm-Alpha Tubulin (TUA1)—A cDNA library from Bmi4 larvae was generated via incubation of isolated mRNA at 45°C for 45 minutes with reverse transcriptase (MMLV-RT from Promega). PCR was carried out using the thermal cycling conditions noted in Jeffries *et al.* [19] at an annealing temperature of 60°C for all amplicons. TUA1 (NM_001043419) was chosen as an endogenous control for the RT-PCR experiments because this protein is ubiquitously expressed throughout the life of *B. mori* [38]. Forward and reverse primers for TUA1 and *Bm*-iAANAT were designed and ordered from Eurofins Genomics and amplify 99 and 119 bp regions respectively, within the open reading frame of the appropriate gene (Table 2). Separate, one-step RT-PCR reactions for TUA1 and *Bm*-iAANAT were prepared. Each RT-PCR reaction solution contained 25 μL of Access Quick Master Mix from Promega, 320 nM forward primer, 320 nM reverse primer, 250 ng fourth instar larval mRNA, 200 units MMLV reverse transcriptase from Promega, and sufficient nuclease-free water to bring the reaction volume to 50 μL. A no reverse transcriptase control was included to confirm the removal of genomic DNA.

2.6.3 Analysis of the cDNA Products—An aliquot (10 μL) of Blue DNA Loading Dye from New England Biolabs (NEB) was added to each cDNA reaction and the resulting 60 μL RT-PCR reaction solutions were loaded into separate lanes of a 1.8% agarose gel containing ethidium bromide. One lane of the gel was loaded with the 100 bp ladder from NEB. Electrophoresis in 1×TAE buffer from NEB (diluted from a 50× stock) allowed for the migration of cDNA products at 50V over a duration of 90 minutes. The cDNA bands (Figure 2) were excised from the gel with a clean razor blade, and the cDNA extracted from the agarose gel slice using the Gel Extraction Wizard from Promega. The isolated cDNA was then sequenced commercially by Eurofins Genomics.

2.7 Extraction and Purification of Fatty Acid Amides from 4th Instar Larvae of B. mori

Bmi4 larvae (3.0 g) were collected on the same day for both mRNA extraction and metabolomic analysis and both collections were carefully assessed to be nearly identical in size and development. The Bmi4 larvae were flash frozen with liquid N_2 and stored at −80°C until after completion of the RT-PCR experiments. The frozen larvae were ground to a paste in 61 mL of methanol using a mortar and pestle and then were homogenized for 5 minutes in a clean, glass beaker using a Heidolph Silent Crusher homogenizer at maximum speed (26,000 rpm). The homogenate was divided into three separate samples of equal mass

and volume into clean, previously unused vials and all were separately re-homogenized for 5 minutes at maximum speed. The fatty acid amides were extracted and purified from these samples using the method of Sultana and Johnson [39], as modified by Jeffries *et al.* [19]. Blanks were prepared and treated exactly in the same manner starting with 61 mL of methanol in a clean mortar and pestle without any addition of Bmi4.

2.8 Identification and Quantitation of Fatty Acid Amides via LC-QToF-MS

2.8.1 Generation of Fatty Acid Amide Standard Curves—With the exception of palmitamide-d_{31}, the fatty acid amides used as internal standards, *N*-arachidonoylglycine-d_8, *N*-arachidonoylethanolamide-d_8, palmitic acid-d_{31}, and *N*-oleoylserotonin-d_{17}, were all from Cayman Chemical. Palmitamide-d_{31} was synthesized from palmitic acid-d_{31} as described [1]. Mass spectral analysis of all the deuterated fatty acid amides, obtained commercially or synthesized in-house, were contaminated by <1% of the corresponding unlabeled fatty acid amide (Figure S1, Supplementary Material). Standard curves were made using pure compounds for each fatty acid amide and internal standards at concentrations ranging from 0.1–10 pmoles in methanol:acetonitrile (1:1) (v/v) per 20 μL injection on the LC-QToF-MS. A mixture was made containing 1 μM of each deuterated standard in methanol:acetonitrile (1:1) (v/v).

2.8.2 Sample Preparation for LC-QToF-MS—The fatty acid amide-containing extracts from Bmi4 larvae were concentrated using 100 μL C_{18} Zip Tips from Thermo Fisher with the following modifications to the manufacturer's recommended protocol: 0.1% (v/v) trifluoroacetic acid (TFA) was substituted for 0.1% TFA: methanol:acetonitrile (8:1:1) (v/v/v) and the fatty acid amides eluted from the tips in 90 μL of acetonitrile:0.1% (v/v) TFA (95:5). The eluent from the Zip Tip was collected in LC vials with spring inserts and 10 μL of the internal standard mixture was added to make a total volume of 100 μL. Samples were analyzed by LC-QToF-MS as described in Section 2.5. The extraction blank was also prepared in the same manner in order to subtract background concentrations of fatty acid amides that may have accrued during the extraction process or unintentionally added from non-deuterated contaminants of the deuterated internal standards.

2.8.3 Identification and Quantification of Fatty Acid Amides in the Bmi4 Extracts—All total ion chromatograms for the Bmi4 larval extracts were scanned for m/z corresponding to fatty acid amides. The retention times and m/z values for metabolites detected in the Bmi4 extracts were compared to those of known standards evaluated under the exact same conditions. The LC column was thoroughly washed (using the same LC method) before the injection of Bmi4 extracts to eliminate false positives. All retention times of detected fatty acid amides were found to be accurate to ± 0.1 minutes of the standard, acceptable deviation of random error from the instrument and the sample matrix effects. These intensity units for each fatty acid amide were converted to pmoles/(gram of tissue) using the standard curves prepared as described in Section 2.8.1.

3. Results

3.1 Cloning, Expression, and Purification of Bm-iAANAT

Bm-iAANAT from *Bombyx mori* was successfully cloned and expressed in *E.coli*. The recombinant *Bm*-iAANAT we designed possessed a his_6-tag on the N-terminus, allowing for a convenient and facile purification by Ni-chelation chromatography. Our yield of purified *Bm*-iAANAT was 17–18 mg of purified protein per liter of *E. coli* culture. Purity was ≥95% as assessed 10% SDS-PAGE gel (Figure S2, Supplementary Material) and the molecular weight from SDS-PAGE analysis was in good agreement with their predicted mass of *Bm*-iAANAT of 29.6 kDa.

3.2 Substrate Specificity of Bm-iAANAT

A screening protocol was used to identify substrates for *Bm*-iAANAT. We pooled together a set of amines (Table S1, Supplementary Material) and evaluated the entire group, at once, for CoA-SH release using a short-chain or long-chain acyl-CoA substrate. The concentration of the individual amines within the pool was high, 60 mM, because of the relatively high K_m (or $K_{m,app}$) value for the amine substrates for some of the GNAT enzymes. For example, the $K_{m,app}$ for glycine for mouse glycine *N*-acyltransferase is 6 mM [40]. A similar protocol could be employed to identify acyl-CoA substrates for *Bm*-AANAT by evaluating groups of acyl-CoA thioesters against an amine co-substrate for CoA-SH releases, but the acyl-CoA thioesters are expensive and long-chain acyl-CoA thioesters can be inhibitors for *N*-acetyltransferases [41,42]. As a compromise, we individually screened the amine pools for CoA-SH release using a short-chain or a long-chain acyl-CoA thioester, acetyl-CoA or oleoyl-CoA, as the acyl donor substrate. The benefits of our screening protocol are clear: any combination of pooled amines and acyl-CoA showing no CoA-SH release activity could be reasonably disregarded for further investigation. A false negative is possible if one of the amines in the pool is a *Bm*-iAANAT inhibitor and the degree inhibition by the inhibitor amine is sufficient to mask CoA-SH release activity from a different amine substrate in the pool. A false negative seems unlikely because the *complete* elimination of CoA-SH release activity would require a balance between [amine inhibitor]/K_i ratio, the [amine substrate]/K_m ratio, and would, most likely, occur if the amine substrate exhibit a low k_{cat} value. Conversely, any combination of pooled amines and acyl-CoA that exhibit CoA-SH release can be investigated individually to define the substrate specificity. The application of our screening protocol to *Bm*-iAANAT revealed significant velocities of CoA-SH release from 5 of the amine pools with acetyl-CoA as the acyl donor and 3 of the amine pools with oleoyl-CoA as the acyl donor (Table S2, Supplementary Material). A significant velocity is defined as any rate of CoA-SH release that is ≥3-fold higher than the background rate of acyl-CoA hydrolysis, 0.1 μmoles/min/mg. The background rate of acyl-CoA hydrolysis was the same, within experimental error, for two controls: no added *Bm*-iAANAT or the reaction initiated by the addition of heat-denatured *Bm*-iAANAT.

In addition to the amine substrates identified by Tsugehara *et al.* [32] (dopamine, octopamine, norepinephrine, serotonin, tryptamine, and tyramine), we found that *Bm*-iAANAT would accept lysine, histamine, alanine, tyramine, ethanolamine, as well as several polyamines (spermidine, agmatine, cadaverine, and putrescine) as substrates. Because of

limited sensitivity of our assay (detection limit of CoA-SH release being ≤ 1 μM), we could not accurately determine the kinetic constants for the remainder of the newly discovered amine substrates for *Bm*-iAANAT with acetyl-CoA as the co-substrate, due to either a low value for either the $K_{m,app}$ or the $k_{cat,app}$. Tsugehara *et al.* [32] employed a more sensitive radiochemical assay with [^{14}C]-acetyl-CoA as a substrate and reported a $K_{m,app}$ value of 0.31 μM for acetyl-CoA.

We repeated the evaluation of the amine pools using oleoyl-CoA as the co-substrate and found that three of the eight amine groups yielded rates of CoA-SH release significantly above background (Table S2, Supplementary Material). Individual interrogation of these groups revealed four amines, tryptamine, tyramine, serotonin, and octopamine, would serve as co-substrates with oleoyl-CoA. With the initial concentration of oleoyl-CoA fixed at 100 μM, tryptamine was the amine with the highest $(k_{cat}/K_m)_{app}$ value, $(1.0 \pm 0.07) \times 10^2$ M^{-1} s^{-1}. Tyramine and octopamine displayed significantly lower $(k_{cat}/K_m)_{app}$ values than tryptamine, attributed both to high $K_{m,app}$ values and lower $k_{cat,app}$ values (Table 3). Qualitatively, the release of CoA-SH was evident when *Bm*-iAANAT was incubated with oleoyl-CoA and serotonin. At the relatively high concentrations of serotonin required to properly measure the formation of *N*-oleoylserotonin, a precipitate formed preventing the accurate quantification of CoA-SH using Ellman's reagent. Thus, we were unable to measure kinetic constants for the *Bm*-iAANAT-catalyzed formation of *N*-oleoylserotonin from serotonin and oleoyl-CoA.

We employed only acetyl- and oleoyl-CoA in our identification of new amine substrates for *Bm*-iAANAT. There are many potential acyl-CoA substrates for *Bm*-iAANAT and we chose to focus on the unbranched, long chain acyl-CoA substrates that are representative of acyl chains found in biologically-occurring fatty acid amides. With tryptamine held at a constant initial concentration of 60 mM, we found that lauroyl-, myristoyl-, palmitoyl-, and arachidonoyl-CoA (all at an initial concentration of 100 μM) were substrates, yielding a rate of CoA-SH release significantly above the background rate of non-enzymatic acyl-CoA hydrolysis. The kinetic constants for these long-chain acyl-CoA substrates are presented in Table 4. We observed a 6.2-fold decrease in the $(k_{cat}/K_m)_{app}$ value as the length of the acyl chain increased from lauroyl-CoA to arachidonoyl-CoA. The decrease in $(k_{cat}/K_m)_{app}$ values was largely a result in a decrease in the $k_{cat,app}$ value because we found the $K_{m,app}$ values were approximately the same for this set of acyl-CoA substrates, ~ 1 μM.

To further explore the observed chain length dependence in the kinetic constants, we determined the kinetic constants for tryptamine while holding the initial concentration of several long-chain acyl-CoA thioesters constant at 100 μM (Table S3, Supplementary Material). We observed a similar pattern in the data. The $(K_{m,\ tryptamine})_{app}$ values are all comparable, ranging from 2.5 mM to 7.0 mM. The $(k_{cat}/K_m)_{tryptamine,\ app}$ was highest when the thioester substrate was lauroryl-CoA and declined ~3-fold as the acyl chain length increased to oleoyl-CoA.

3.3 Product Characterization of a Bm-iAANAT-Catalyzed Reaction

The use of Ellman's reagent to detect CoA-SH release does not prove *Bm*-iAANAT has catalyzed the formation of an *N*-acylamide from an acyl-CoA and an amine. While unlikely,

CoA-SH release could reflect the amine activation of *Bm*-iAANAT-catalyzed thioester hydrolysis: CoA-S-CO-R + H_2O → R-COOH + CoA-SH. We compared a synthetic standard of *N*-oleoyltryptamine against the product generated by the incubation of *Bm*-iAANAT with tryptamine and oleoyl-CoA. The analysis of the enzymatic product corroborated our kinetic data: the *N*-oleoyltryptamine produced by *Bm*-iAANAT catalysis is consistent with the $[M+H]^+$ peak and retention time (±0.2 minutes reported error for the LC-QToF-MS) vs. the *N*-oleoyltryptamine standard (Table 5). We did not detect any compounds with the retention time or m/z of *N*-oleoyltryptamine in the no enzyme-containing (blank) samples.

3.4 Detection of Bm-iAANAT Transcript in 4th Instar Larvae of B. mori via RT-PCR

Our *in vitro* studies of purified, recombinant *Bm*-iAANAT suggest this enzyme could have a role in the biosynthesis of fatty acid amides. Our next steps were to determine if fatty acid amides are produced by *B. mori* and, if so, does the presence of these molecules in *B. mori* correlate, at all, to the expression of *Bm*-iAANAT. We identified the presence of *Bm*-iAANAT transcripts by RT-PCR. Primers were prepared to generate a 119 bp *Bm*-iAANAT-derived RT-PCR product and a 99 bp *Bm*-TUA1-derived product (as a control) from a 4th instar larvae *B. mori* cDNA library.

After the migration of cDNA products on an agarose gel containing ethidium bromide, the gel was viewed under UV light to illuminate the RT-PCR products. The RT-PCR products match the expected sizes for the *Bm*-iAANAT and *Bm*-TUA1 transcripts, respectively (Fig. 2).

3.5 Detection of a Panel of Fatty Acid Amides from Bmi4 via LC-QToF-MS

All total ion chromatograms (TIC) for the 4th instar larvae were scanned for m/z similar to the fatty acid amides found in *D. melanogaster* [19]. The retention times and m/z values for metabolites detected in the Bmi4 extracts were compared to those of known standards evaluated under the exact same conditions. The intensities for the m/z values corresponding to a specific fatty acid amide were converted to pmoles/(gram of tissue) based on standard curves prepared with corresponding authentic fatty acid amide. The fatty acid amides identified from Bmi4 larvae are shown in Table 6.

4. Discussion and Conclusions

In this study, we have successfully cloned, expressed, purified, and characterized *Bm*-iAANAT, an arylalkylamine *N*-acyltransferase from *Bombyx mori*. The characterization of *Bm*-iAANAT contributes to the body of knowledge leading to a pest-specific iAANAT inhibitor, important because iAANATs are suggested as new targets for the development of insecticides [43–46]. The most important finding from our work was that *Bm*-iAANAT will accept long-chain acyl-CoA thioesters as substrates. This result coupled to our demonstration that the enzyme is expressed in 4th instar larvae and to our identification of fatty acid amides in the 4th instar larvae of *B. mori* suggests, but does not prove, *Bm*-iAANAT has a role in the biosynthesis of, at least, a few members of the fatty acid amide family in this insect. We have long thought an acyltransferase could function in fatty acid

amide production *in vivo* [25]. *Bm*-iAANAT is one of few known acyl-CoA-dependent transferases accepting fatty acyl-CoA thioesters as substrates for the enzymatic production of fatty acid amides; the others being human glycine *N*-acyltransferase like-2 [29], human glycine *N*-acyltransferase like-3 [24], and *D. melanogaster* arylalkylamine *N*-acyltransferase like-2 (AANATL2) [23]. In addition, *N*-myristoyltransferase (NMT) utilizes myristoyl-CoA as the myristoyl donor for the myristoylation of the N-terminus of proteins [28]. The direct conjugation of an amine to unactivated fatty acid, while thermodynamically unfavorable under biological conditions, has been attributed to the biosynthesis of fatty acid amides [47,48]. This includes the conjugation of linolenic acid to L-glutamine to yield *N*-linolenoyl-L-glutamine in the caterpillars of *Manduca sexta* [49].

Based on our current understanding of the substrate specificity of *Bm*-iAANAT (Tables 3 and 4 and ref. [32]) and the fatty acid amides identified in Bmi4 (Table 6), *Bm*-iAANAT could serve *in vivo* to generate the *N*-fatty acyl -serotonins and -dopamines. The possibility of *Bm*-iAANAT having a broader role in the biosynthesis of other *N*-fatty acylamides, based on its amine specificity, awaits further work: the identification of other *N*-fatty acylamides in *B. mori* and/or alternations in the fatty acid amidome after the knock down of *Bm*-iAANAT expression. The CRISPR/cas9 system has been used in *B. mori* for the targeted elimination of a protein [50,51]. We used targeted knockdown methods to demonstrate the glycine *N*-acyltransferase like-3 and peptidylglycine α-amidating monooxygenase function sequentially in mouse neuroblastoma $N_{18}TG_2$ cells to convert fatty acyl-CoA thioesters to the fatty acid primary amides [24].

Another interesting outcome from our work on *Bm*-iAANAT is the influence that acyl-CoA substrate chain length has on the affinity of the enzyme for the amine substrate. $K_{m,app}$ values are not $K_{dissociation}$ values and a discussion of the affinity of *Bm*-iAANAT for the amine substrates assumes that differences in $K_{m,app}$ values for the amines does, at least, approximate the influence of the acyl-CoA substrate on the $K_{dissociation}$ values for an amine. Our work and that of Tsugehara *et al*. [32] show low $K_{m,app}$ values for the amine substrates when acetyl-CoA is the acyl donor. The $K_{m,app}$ value for tryptamine increases >1,000-fold when the acyl-CoA donor has an acyl chain of 12 carbons or longer (lauroyl-CoA to oleoyl-CoA) (Table 4). We have observed similar trends for other iAANATs, but the effect is more pronounced for *Bm*-iAANAT. For *D. melanogaster* AANATL7, we found the $K_{m,app}$ for histamine increased from 0.52 mM when acetyl-CoA was the acyl donor to 15 mM when hexanoyl-CoA was the acyl donor [42]. For *D. melanogaster* AANATL2, the $K_{m,app}$ for serotonin increased from 7.2 μM for acetyl-CoA to 870 μM for palmitoyl-CoA [23]. We have recently shown the acetyl group of acetyl-CoA shifts the conformational ensemble of *Bm*-iAANAT3 to a high affinity, catalytically efficient conformation [52]. The data presented here on *Bm*-iAANAT is consistent with this conclusion and clearly demonstrates that a long acyl chain in the acyl-CoA hinders the most effective positioning of the amine for nucleophilic attack at the thioester bond of the acyl-CoA. A more precise understanding of conformational dynamics and the effects of dynamics on substrate positioning and catalysis in the iAANATs requires structural information. *Bm*-iAANAT could prove the better enzyme in addressing these questions because the amine affinity is more strongly influenced by the length of the acyl chain in the acyl-CoA than in other iAANATs.

Our identification of fatty acid amides in Bmi4 is the first report of these lipid amides in *B. mori*. Long-chain fatty acids are known in *B. mori* [53–56] and the only report of a related *N*-acylamide in *B. mori* is *N*-acetylglutamate [56]. Fatty acid amides have a long and underappreciated history in insects, starting with the discovery of volicitin, *N*-(17-hydroxylinolenoyl)-L-glutamine, from *Spodoptera exigua* [15]. Volicitin, volicitin analogs, and other fatty acid amides have been reported in insects other than *B. mori*, including *D. melanogaster* [16–20]. The function for most of the fatty acid amides in insects (and many other organisms) remains elusive. The apparent lack of the cannabinoid receptors in *D. melanogaster* [21] despite reports of endocannabinoid-like fatty acid amides in *D. melanogaster* [17–19] hints that fatty acid amides serve a different role in insects (and other invertebrates) relative to their functions in vertebrates. This points to a fascinating evolutionary story for these molecules as vertebrates emerged from invertebrates.

Supplementary Material

Refer to Web version on PubMed Central for supplementary material.

Acknowledgments

This work has been supported, in part, by grants from the University of South Florida (a Creative Scholarship grant), the Shirley W. and William L. Griffin Charitable Foundation, the National Institute of Drug Abuse at the National Institutes of Health (R03-DA034323) and the National Institute of General Medical Science of the National Institutes of Health (R15-GM107864) to D.J.M. This work has also received support from the Mass Spectrometry and Peptide Facility, Department of Chemistry, University of South Florida. The authors thank Sydney Balgo for technical assistance with some of the research and Dr. Ioannis Gelis for many helpful discussions throughout this work.

References

1. Farrell EK, Chen Y, Barazanji M, Jeffries KA, Cameroamortegui F, Merkler DJ. Primary fatty acid amide metabolism: conversion of fatty acids and an ethanolamine in $N_{18}TG_2$ and SCP cells. J Lipid Res. 2012; 53:247–256. DOI: 10.1016/j.drudis.2008.02.006 [PubMed: 22095832]
2. Iannotti FA, Di Marzo V, Petrosino S. Endocannabinoids and endocannabinoid-related mediators: Targets, metabolism and role in neurological disorders. Prog Lipid Res. 2016; 62:107–128. DOI: 10.1016/j.plipres.2016.02.002 [PubMed: 26965148]
3. Witkamp R. Fatty acids, endocannabinoids, and inflammation. Eur J Pharmacol. 2016; 785:96–107. DOI: 10.1016/j.ejphar.2015.08.051 [PubMed: 26325095]
4. Ure A. Gouty concretions, with a new method of treatment. Med Chir Trans. 1841; 24:30–35.
5. Keller W. Ueber verwandlung der benzoësäure in hippursäure. Justus Liebigs Ann Chem. 1842; 43:108–111.
6. Spillane JD. A memorable decade in the history of neurology 1874–84-II. Br Med J. 1974; 4:757–759. [PubMed: 4613426]
7. Devane WA, Hanuš L, Breuer A, Pertwee RG, Stevenson LA, Griffin G, Gibson D, Mandelbaum A, Etinger A, Mechoulam R. Isolation and structure of a brain constituent that binds to the cannabinoid receptor. Science. 1992; 258:1946–1949. http://doi:10.1126/science.1470919. [PubMed: 1470919]
8. Hua T, Vemuri K, Pu M, Qu L, Han GW, Wu Y, Zhao S, Shui W, Li S, Korde A, Laprairie RB, Stahl EL, Ho J-H, Zvonok N, Zhou H, Kufareva I, Wu B, Zhao Q, Hanson MA, Bohn LM, Makriyannis A, Stevens RC, Liu Z-J. Crystal structure of the human cannabinoid receptor r. Cell. 2016; 167:750–762. DOI: 10.1016/j.cell.2016.10.004 [PubMed: 27768894]
9. Maccarrone M, Bab I, Bíró T, Cabral GA, Dey SK, Di Marzo V, Konje JC, Kunos G, Mechoulam R, Pacher P, Sharkey KA, Zimmer A. Endocannabinoid signaling at the periphery: 50 years after THC.

Trends Pharmacol Sci. 2015; 36:277–296. http://doi:10.1016/j.tips.2015.02.008. [PubMed: 25796370]

10. Lu H-C, Mackie K. An introduction to the endogenous cannabinoid system. Biol Psychiatry. 2016; 79:516–525. DOI: 10.1016/j.biopsych.2015.07.028 [PubMed: 26698193]
11. Fezza F, Bari M, Florio R, Talamonti E, Feole M, Maccarrone M. Endocannabinoids, related compounds and their metabolic routes. Molecules. 2014; 19:17078–17106. http://doi:10.3390/molecules191117078. [PubMed: 25347455]
12. Cravatt BF, Prospero-Garcia O, Siuzdak G, Gilula NB, Henriksen SJ, Boger DL, Lerner RA. Chemical characterization of a family of brain lipids that induce sleep. Science. 1995; 268:1506–1509. http://doi:10.1126/science.7770779. [PubMed: 7770779]
13. Schmid PC, Krebsbach RJ, Perry SR, Dettmer TM, Maasson JL, Schmid HHO. Occurrence and postmorten generation of anandamide and other long-chain *N*-acylethanolamines in mammalian brain. FEBS Lett. 1995; 375:117–120. http://doi:10.1016/0014-5793(95)01194-J. [PubMed: 7498458]
14. Maccrrone M, Attinà M, Cartoni A, Bari M, Finazzi-Agrò A. Gas chromatography-mass spectrometry analysis of endogenous cannabinoids in healthy and tumoral human brain and human cells in culture. J Neurochem. 2001; 76:594–601. http://doi:10.1046/j.1471-4159.2001.00092.x. [PubMed: 11208922]
15. Alborn HT, Turlings TCJ, Jones TH, Stenhagen G, Loughrin JH, Tumlinson JH. An elicitor of plant volatiles from beet armyworm oral secretion. Science. 1997; 276:945–949. http://doi:10.1126/science.276.5314.945.
16. Fezza F, Dillwith JW, Bisogno T, Tucker JS, Di Marzo V, Sauer JR. Endocannabinoids and related fatty acid amides, and their regulation, in the salivary gland of the lone star tick. Biochim Biophys Acta. 2003; 1633:61–67. http://doi:10.1016/S1388-1981(03)00087-8. [PubMed: 12842196]
17. Yoshinaga N, Aboshi T, Ishikawa C, Fukui M, Shimoda M, Nishida R, Lait CG, Tumlinson JH, Mori N. Fatty acid amides, previously identified in caterpillars, found in the cricket *Teleogryllus taiwanemma* and fruit fly *Drosophila melanogaster* larvae. J Chem Ecol. 2007; 33:1376–1381. http://doi10.1007/s10886-007-9321-2. [PubMed: 17566833]
18. Tortoriello G, Rhodes BP, Takacs SM, Stuart JM, Basnet A, Raboune S, Widlanski TS, Doherty P, Harkany T, Bradshaw HB. Targeted lipidomics in *Drosophila melanogaster* identifies novel 2-monoacylglycerols and *N*-acyl amides. PLoS One. 2013; 8:e67865.doi: 10.1371/journal.pone.0067865 [PubMed: 23874457]
19. Jeffries KA, Dempsey DR, Behari AL, Anderson RL, Merkler DJ. *Drosophila melanogaster* as a model system to study long-chain fatty acid amide metabolism. FEBS Lett. 2014; 588:1596–1602. http://doi:10.1016/j.febslet.2014.02.051. [PubMed: 24650760]
20. Yoshinaga N, Ishikawa C, Seidl-Adams I, Bosak E, Aboshi T, Tumlinson JH, Mori N. *N*-(18-Hydroxylinolenoyl)-L-glutamine: A newly discovered analog of volicitin in *Manduca sexta* and its elcitior activity in plants. J Chem Ecol. 2014; 40:484–490. http://doi:10.1007/s10886-014-0436-y. [PubMed: 24817386]
21. McPartland J, Di Marzo V, De Petrocellis L, Mercer A, Glass M. Cannabinoid receptors are absent in insects. J Comp Neurol. 2001; 436:423–429. http://doi:10.1002/cne.1078. [PubMed: 11447587]
22. Waluk DP, Battistini MR, Dempsey DR, Farrell EK, Jeffries KA, Mitchell P, Hernandez LW, McBride JC, Merkler DJ, Hunt MC. Mammalian fatty acid amides of the brain and CNS. In: Watson RR, DeMeester F, editorsOmega-3 Fatty Acids in Brain and Neurological Health. Academic Press; London: 2014. 87–107. http://doi:10.1016/B978-0-12-410527-0.00009-0
23. Dempsey DR, Jeffries KA, Anderson RL, Carpenter A-M, Rodriguez Ospina SDJ. Identification of an arylalkylamine *N*-acyltransferase from *Drosophila melanogaster* that catalyzes the formation of long-chain *N*-acylserotonins. FEBS Lett. 2014; 588:594–599. http://doi:10.1016/j.febslet.2013.12.027. [PubMed: 24444601]
24. Jeffries KA, Dempsey DR, Farrell EK, Anderson RL, Garbade GJ, Gurina TS, Gruhonjic I, Gunderson CA, Merkler DJ. Glycine *N*-acyltransferase-like 3 is responsible for long-chain *N*-acylglycine formation in $N_{18}TG_2$ cells. J Lipid Res. 2016; 57:781–790. http://doi:10.1194/jlr.M062042. [PubMed: 27016726]

25. Merkler DJ, Merkler KA, Stern W, Fleming FF. Fatty acid amide biosynthesis: A possible new role for peptidylglycine α-amidating enzyme and acyl-coenzyme A:glycine *N*-acyltransferase. Arch Biochem Biophys. 1996; 330:430–434. http://doi:10.1006/abbi.1996.0272. [PubMed: 8660675]
26. Vetting MW, de Carvalho LPS, Yu M, Hegde SS, Magnet S, Roderick SL, Blanchard JS. Structure and functions of the GNAT superfamily of acetyltransferases. Arch Biochem Biophys. 2005; 433:212–226. http://doi:10.1016/j.abb.2004.09.003. [PubMed: 15581578]
27. Ud-Din AI, Tikhomirova A, Roujeinikova A. Structure and functional diversity of GCN5-related *N*-acetyltransferases. Int J Mol Sci. 2016; 17 pii: E1018, http://doi:10.3390/ijms17071018.
28. Rajala RVS, Datla RSS, Moyana RN, Kakkar R, Carlsen SA, Sharma RK. N-myristoyltransferase. Mol Cell Biochem. 2000; 204:135–155. http://doi:10.1023/A:1007012622030. [PubMed: 10718634]
29. Waluk DP, Schultz N, Hunt MC. Identification of glycine *N*-acyltransferase-like 2 (GLYATL2) as a transferase that produces *N*-acyl glycines in humans. FASEB J. 2010; 24:2795–2803. http://doi:10.1096/fj.09-148551. [PubMed: 20305126]
30. Di Marzo V, De Petrocellis L, Sepe N, Buono A. (1996) Biosynthesis of anandamide and related acylethanolamides in mouse J774 macrophages and N_{18} neuroblastoma cells. Biochem J. 1996; 316:977–984. http://doi:10.1042/bj3160977. [PubMed: 8670178]
31. Bisogno T, Sepe N, De Petrocellis L, Mechoulam R, Di Marzo V. The sleep inducing factor oleamide is produced by mouse neuroblastoma cells. Biochem Biophys Res Commun. 1997; 239:473–479. http://doi:10.1006/bbrc.1997.7431. [PubMed: 9344854]
32. Tsugehara T, Iwai S, Fujiwara Y, Mita K, Takeda M. Cloning and characterization of insect arylalkylamine *N*-acetyltransferase from *Bombyx mori*. Comp Biochem Physiol B Biochem Mol Biol. 2007; 147:358–366. http://doi:10.1016/j.cbpb.2006.10.112. [PubMed: 17449311]
33. Zhan S, Guo Q, Li M, Li M, Li J, Miao X, Huang Y. Disruption of an N-acetyltransferase gene in silkworm reveals a novel role in pigmentation. Development. 2010; 137:4083–4090. http:/doi:10.1242/dev.053678. [PubMed: 21062865]
34. Dai F-yQiao L, Tong X-lCao C, Chen P, Chen J, Lu C, Xiang Z-h. Mutations of an arylalkylamine-*N*-acetyltransferase, *Bm*-iAANAT, are responsible for silkworm melanism mutant. J Biol Chem. 2010; 285:19553–19560. http://doi:10.1074/jbc.M109.096743. [PubMed: 20332088]
35. Grudmann F, Dill V, Dowling A, Thanwisai A, Bode E, Chantratitia N, ffrench-Constant R, Bode HB. (2012) Identification and isolation of insecticidal oxazoles from *Pseudomonas* spp. Beilstein J Org Chem. 2012; 8:749–752. http://doi:10.3762/bjoc.8.85. [PubMed: 23015823]
36. Ellman GL. Tissue sulfhydryl groups. Arch Biochem Biophys. 1959; 82:70–77. http://doi:10.1016/0003-9861(59)90090-6. [PubMed: 13650640]
37. Barrante JR. Applied Mathematics for Physical Chemistry:Third Edition. Pearson Prentice Hall; Upper Saddle River, NJ: 2004.
38. Kawasaki H, Sugaya K, Quan G-X, Nohata J, Mita K. Analysis of α- and β-tubulin genes of *Bombyx mori* using an EST database. Insect Biochem Mol Biol. 2003; 33:131–137. DOI: 10.1016/S0965-1748(02)00184-4 [PubMed: 12459208]
39. Sultana T, Johnson ME. Sample preparation and gas chromatography of primary fatty acid amides. J Chromatogr A. 2006; 1101:278–285. DOI: 10.1016/j.chroma.2005.10.0273 [PubMed: 16266715]
40. Dempsey DR, Bond JD, Carpenter A-M, Rodriguez Ospina S, Merkler DJ. Expression, purification, and characterization of mouse glycine *N*-acyltransferase in *Escherichia coli*. Protein Expr Purif. 2014; 97:23–28. DOI: 10.1016/j.pep.2014.02.007 [PubMed: 24576660]
41. Dempsey DR, Jeffries KA, Bond JD, Carpenter A-M, Rodriguez-Ospina S, Breydo L, Caswell KK, Merkler DJ. Mechanistic and structural analysis of *Drosophila melanogaster* arylalkylamine N-acetyltransferases. Biochemistry. 2014; 53:7777–7793. DOI: 10.1021/bi5006078 [PubMed: 25406072]
42. Dempsey DR, Jeffries KA, Handa S, Carpenter A-M, Rodriguez-Ospina S, Breydo L, Merkler DJ. Mechanistic and structural analysis of a *Drosophila melanogaster* enzyme, arylalkylamine *N*-acetyltransferase like 7, an enzyme that catalyzes the formation of *N*-acetylarylakylamides and *N*-acetylhistamine. Biochemistry. 2015; 54:2644–2658. http://doi:10.1021/acs.biochem.5b00113. [PubMed: 25850002]

43. O'Flynn BG, Hawley AJ, Merkler DJ. Insect Arylalkylamine *N*-Acetyltransferases as Potential Targets for Novel Insecticide Design. Biochem Mol Biol J. 2018; 4 pii, http://doi:10.21767/2471-8084.100053.
44. Han Q, Robinson H, Ding H, Christensen BM, Li J. Evolution of insect arylalkylamine *N*-acetyltransferases: Structural evidence from yellow fever mosquito, *Aedes aegypti*. Proc Natl Acad Sci USA. 2012; 109:11669–11674. http://doi:10.1073/pnas/1206828109. [PubMed: 22753468]
45. Tsugehara T, Imai T, Takeda M. Characterization of arylalkylamine *N*-acetyltransferase from silkmoth (*Antheraea pernyi*) and pesticidal drug edesign base on the baculovirus-expressed enzyme. Comp Biochem Physiol C Toxicol Pharmacol. 2013; 157:93–102. http://doi:10.1016/j.cbpc.2012.10.003. [PubMed: 23064182]
46. Lourenço BLA, Silva MVAS, deOliveira EB, de Assis Soares WR, Góes-Neto A, Santos G, Andrade BS. Virtual screening and molecular docking for arylalkylamine-N-acetyltransferase (aaNAT) inhibitors, a key enzyme of *Aedes* (Stegomyia) *aegypti* (L.) metabolism. Comput Mol Biosci. 2015; 5:35–44. DOI: 10.4236/cmb.2015.53005
47. Bachur NR, Udenfriend S. Microsomal synthesis of fatty acid amides. J Biol Chem. 1966; 241:1308–1313. [PubMed: 5935346]
48. Arreaza G, Devane WA, Omeir RL, Sajnani G, Kunz J, Cravatt BF, Deutsch DG. The cloned rat hydrolytic enzyme responsible for the breakdown of anandamide also catalyzes it formation via the condensation of arachidonic acid and ethanolamine. Neurosci Lett. 1997; 234:59–62. DOI: 10.1016/S0304-3940(97)00673-3 [PubMed: 9347946]
49. Lait CG, Alborn HT, Teal PEA, Tumlinson JH III. Rapid biosynthesis of *N*-linolenoyl-L-glutamine, an elicitor of plant volatiles, by membrane-associated enzyme(s) in *Manduca sexta*. Proc Natl Acad Sci USA. 2003; 100:7027–7032. http://doi:10.1073/pnas.1232474100. [PubMed: 12773625]
50. Ma S, Chang J, Wang X, Liu Y, Zhang J, Lu W, Gao J, Shi R, Zhao P, Xia Q. CRISPR/Cas9 medicated multiplex genome editing and heritable mutagenesis of *BmKu70* in *Bombyx mori*. Sci Rep. 2014; 4:4489. http://doi:10.1038/srep04489. [PubMed: 24671069]
51. Liu Y, Ma S, Chang J, Zhang T, Wang X, Shi R, Zhang J, Lu W, Liu Y, Xia Q. Tissue-specific genome editing of laminA/C in the posterior silk glands of *Bombyx mori*. J Genet Genomics. 2017; 44:451–459. DOI: 10.1016/j.jgg.2017.09.003 [PubMed: 28967614]
52. Aboalroub AA, Bachman AB, Zhang Z, Keramisanou D, Merkler DJ, Gelis I. Acetyl group coordinated progression through the catalytic cycle of an arylalkylamine N-acetyltransferase. PLoS One. 2017; 12:e0177270.doi: 10.1371/journal.pone.0177270 [PubMed: 28486510]
53. Kwon M-G, Kim D-S, Lee J-H, Park S-W, Choo Y-K, Han Y-S, Kim J-S, Hwang K-A, Ko K, Ko K. Isolation and analysis of natural compounds from silkworm pupae and effect of its extracts on alcohol detoxification. Entomol Res. 2012; 42:55–62. http://doi:10.1111/j.1748-5967.2011.00439.x.
54. Paul D, Dey S. Essential amino acids, lipid profile and fat-soluble vitamins of the edible silkworm *Bombyx mori* (Lepidoptera: Bombycidae). Int J Trop Insect Sci. 2014; 34:239–247. http://doi:10.1017/S1742758414000526.
55. Zhou L, Li H, Hao F, Li N, Liu X, Wang G, Wang Y, Tang H. Developmental changes for the hemolymph metabolome of silkworm (*Bombyx mori* L.). J Proteome Res. 2015; 14:2331–2347. http://doi:10.1021/acs.jproteome.5b00159. [PubMed: 25825269]
56. Li Y, Chen Q, Hou Y, Xia Q, Zhao P. Metabolomic analysis of the larval head of the silkworm, *Bombyx mori*. Int J Mol Sci. 2016; 17:1460. http://doi:10.3390/ijms17091460.

Highlights

- An enzyme in silkworms was found to be capable of synthesizing cannabinoid-like molecules.
- Cannabinoid-like signaling molecules were quantified in silkworms for the first time.
- *Bm-iAANAT* transcripts were identified in the 4th instar of *B. mori.*

SUMMARY

Herein, we detail the successful expression, purification, and characterization of an arylalkylamine *N*-acyltransferase from *Bombyx mori* (*Bm*-iAANAT) in *E. coli*. Our *in vitro* determination of substrate specificity for *Bm*-iAANAT demonstrates that this enzyme will accept long-chain fatty acyl-CoA thioesters as substrates leading to the formation of long chain *N*-acylarylalkylamides. In addition, we show that *Bm*-iAANAT is, most likely, responsible for the *in vivo* biosynthesis of such metabolites in *B. mori* due to the detection of the *Bm*-iAANAT transcripts along with the identification and quantification of several long chain *N*-acylarylalkylamides and other long chain fatty acid amides in *B. mori*.

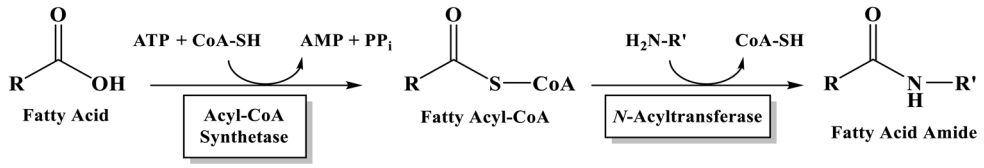

Figure 1.

Proposed Role of *N*-Acyltransferases in Fatty Acid Amide Biosynthesis

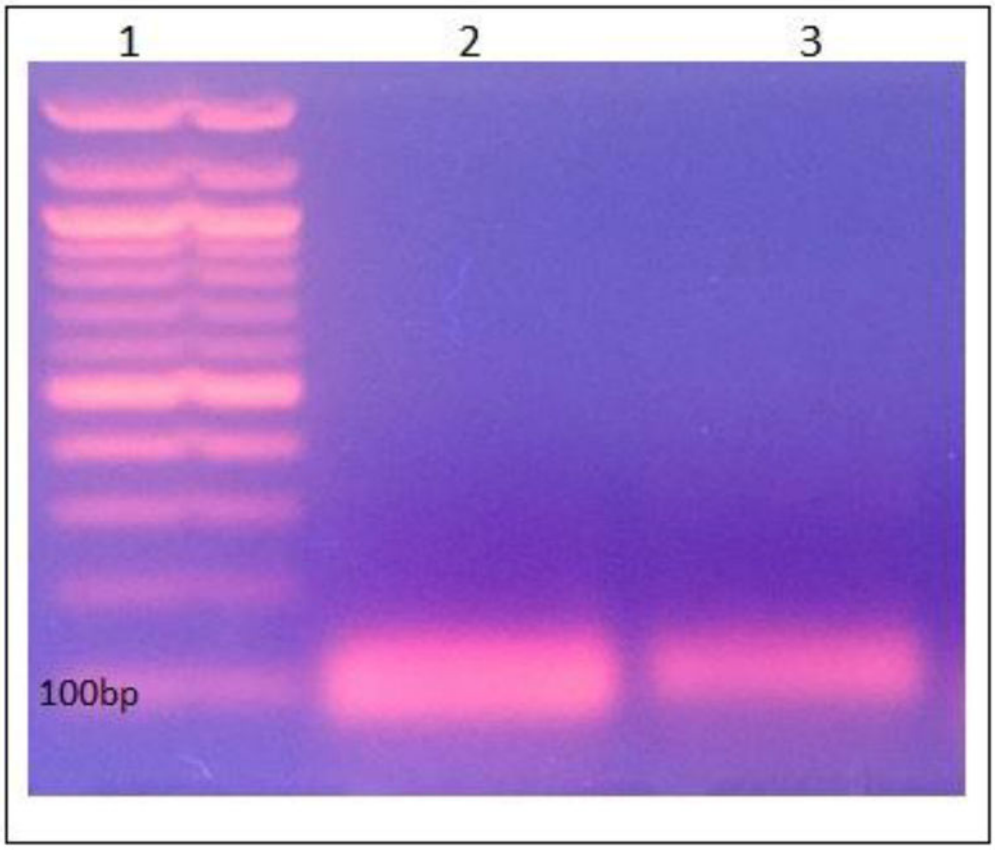

Figure 2.

RT-PCR of *Bm*-iAANAT and *Bm*-TUA1 in the 4th Instar of *B. mori*. Lane 1 contains 100 bp ladder; the band on the bottom denotes 100 bp standard. Lane 2 was loaded with the RT-PCR product for *Bm*-TUA1 (99 bp). Lane 3 was loaded with RT-PCR product for *Bm*-iAANAT (119 bp). The amplicon product extracted from lane 2 matched the sequence for *Bm*-TUA1, while the amplicon product extracted from lane 3 matched the sequence for *Bm*-iAANAT.

Table 1

Method for the DNase I-mediated Degradation of Genomic DNA

Reagent	Recommended Protocol[a]	Modified Protocol
mRNA	1 μg	1 μg
DNase I	1 μL	2 μL
DNase I Buffer with $MgCl_2$	1 μL	2 μL
Nuclease-Free Water	to 10 μL	to 18 μL

[a] As recommended by the manufacturer.

Table 2

Primers Used to Amplify TUA1 and *Bm*-iAANAT

Primer	Primer Sequence
TUA 1 Forward Primer	AGATGCCCACAGACAAGACC
TUA 1 Reverse Primer	CAAGATCGACGAAGAGAGCA
Bm-iAANAT Forward Primer	CAAAATGTCCGTTCCAGCTT
Bm-iAANAT Forward Primer	GATTGACGGCGAGATTCATT

Table 3

Steady-state Kinetic Constants for Different Amine Substrates with Oleoyl-CoA as the Acyl Donor[a,b]

Amine[c]	$K_{m,app}$ (mM)	$k_{cat,app}$ (s^{-1})	$(k_{cat}/K_m)_{app}$ (M^{-1} s^{-1})
Tryptamine	7.0 ± 0.5	0.72 ± 0.01	(1.0 ± 0.07) × 10^2
Tyramine	84 ± 12	2.7 ± 0.19	32 ± 5.3
Octopamine	65 ± 16	0.31 ± 0.04	4.7 ± 1.2

[a] Reaction conditions were 300 mM Tris pH 8.0, 150 μM DTNB, 100 μM oleoyl-CoA, and varied initial concentrations of the indicated amine.

[b] Kinetic constants are reported with the standard error (n = 3).

[c] Serotonin is an amine substrate when oleoyl-CoA is the acyl donor. However, a precipitate formed during catalysis which interfered with the assay and prevented the accurate determination of the kinetic constants for serotonin.

Table 4

Steady-state Kinetic Constants for Long-Chain Acyl-CoA Substrates with Tryptamine as the Acyl Acceptor[a,b]

Acyl-CoA	$K_{m,app}$ (μM)	$k_{cat,app}$ (s^{-1})	$(k_{cat}/K_m)_{app}$ (M^{-1} s^{-1})
Lauroyl-CoA	0.97 ± 0.12	1.3 ± 0.01	$(1.4 \pm 0.2) \times 10^5$
Myristoyl-CoA	0.92 ± 0.20	0.66 ± 0.01	$(7.2 \pm 1.5) \times 10^5$
Palmitoyl-CoA	1.1 ± 0.30	0.51 ± 0.01	$(4.9 \pm 1.4) \times 10^5$
Oleoyl-CoA	1.7 ± 0.51	0.42 ± 0.02	$(2.4 \pm 0.70) \times 10^5$
Arachidonoyl-CoA	1.2 ± 0.67	0.27 ± 0.02	$(2.4 \pm 1.3) \times 10^5$

[a] Reaction conditions were 300 mM Tris pH 8.0, 150 μM DTNB, 60 mM tryptamine, and varied initial concentrations of the acyl-CoA.

[b] Kinetic constants are reported with the standard error (n = 3).

Table 5

Characterization of the *Bm*-iAANAT-catalyzed reaction via LC-QTOF-MS analysis

Sample	Retention Time (min)	$[M+H]^+$ (m/z)
N-Oleoyltryptamine Standard	6.489	425.2588
Bm-iAANAT Product	6.503	425.2574

Table 6

Fatty Acid Amides Detected in 4th Instar Larvae of *B. mori*

Fatty Acid Amide	Standard (m/z)	4th Instar (m/z)	Standard (Retention time)	4th Instar (Retention time)	Amount Extracted (pmoles/g)[a]
Palmitamide	256.2645	256.2631	6.214 min.	6.213 min.	28 ± 19
N-Palmitoylserotonin	415.3322	415.2882	6.187 min.	6.125 min.	9.8 ± 0.6
Palmitoleamide	254.2456	254.2463	5.857 min.	5.859 min.	22 ± 13
N-Stearoylserotonin	443.3638	443.3505	6.542 min.	6.576 min.	1.1 ± 0.4
Oleamide	282.2796	282.2786	6.289 min.	6.277 min.	33 ± 2.9
N-Oleoyldopamine	418.3315	418.3306	6.248 min.	6.246 min	6.0 ± 0.3
N-Oleoylethanolamine	326.3057	3.26.3049	6.077 min.	6.074 min	20 ± 15
N-Oleoylglycine	340.2846	340.2847	6.094 min.	5.945 min.	14 ± 1.5
N-Oleoylserotonin	441.3479	441.3483	6.262 min.	6.322 min	3.5 ± 0.6
Linoleamide	280.2643	280.2616	5.979 min.	6.027 min.	22 ± 14
N-Arachidonoylserotonin	463.3326	463.3337	6.071 min.	6.069 min.	14 ± 2.9

[a]Average ± standard deviation for 3 separate measurements.